www.czasopisma.pan.pl PAN POLSKA AKADEMIA NAUK www.journals.pan.pl

Arch. Metall. Mater., Vol. 61 (2016), No 3, p. 1379–1384

DOI: 10.1515/amm-2016-0226

W. HABRAT*, M. MOTYKA**, K.TOPOLSKI***, J. SIENIAWSKI**

EVALUATION OF THE CUTTING FORCE COMPONENTS AND THE SURFACE ROUGHNESS IN THE MILLING PROCESS OF MICRO- AND NANOCRYSTALLINE TITANIUM

Abstract: Nanocristalline pure titanium in comparison to microcrystalline titanium is characterized by better mechanical properties which influence its wider usability. The aim of the research was to evaluate whether the grain size of pure titanium (micro- and nanocrystalline) has influence on the cutting force components and the surface roughness in the milling process. Models of cutting force components for both materials were prepared and differences between the results were examined. The feed rate effect on selected parameters of surface roughness after milling of micro- and nanocrystalline pure titanium was determined.

Keywords: nanocrystalline titanium, hydrostatic extrusion, cutting force, surface roughness, milling

1. Introduction

Development of severe plastic deformation (SPD) methods allows to obtain the titanium with nanocrystalline grains. Grain refinement in pure titanium results in improvement of its mechanical properties [1]. Nanocrystalline pure titanium have three times higher strength than the microcrystalline one. Its mechanical properties are comparable to widely used Ti-6Al-4V alloy [2]. Due to the unique properties of titanium and its alloys like thermal conductivity and elastic modulus, high hardness at elevated temperature and high chemical reactivity at low density, these materials are difficult to machine [3]. These factors may cause rapid tool wear, low material removal rate and degradation of surface integrity of machined parts [4-5]. The cutting force components and surface roughness are the main parameters providing information on machinability of materials [6-9]. It is expected that machinability of nanocrystalline titanium is changed mainly due to work hardening caused by grain refinement. In titanium alloys work hardening during machining eliminates formation of built-up edge in front of the cutting tool and increase of the shearing angle. As a consequence the thin chips contact a relatively small area in the cutting face, resulting in high bearing loads per unit area. For this case the friction between the chip and bearing area causes significant heat increase in a very small area of the cutting tool and formation of cratering close to the cutting edge leading to rapid tool breakdown [10-12].

The specific properties of nanocrystalline titanium allows its use in medicine. Nanocrystalline titanium could be used for the production of e.g. dental implants. Some titanium alloys used in medicine contain toxic elements, such as vanadium. Therefore, from a biological point of view it is preferable to use implants made of pure titanium [13]. Obtaining information on process quality indicators is a way of supporting decisions in the design stage: tool life, surface roughness, state of technological surface layer [14], chip control and cutting force compnents [15].

Extensive research work has been done on machining of titanium and its alloys [16,17] taking into account modelling and simulation of this process [18,19]. However only a few papers are related to ultrafine-grained titanium [20]. Therefore, it is necessary to acquire knowledge in the field of machining of nanocrystalline titanium. The comparison of test results on micro- and nanocrystalline titanium allows to check whether the grain size of pure titanium has influence on the cutting force components and the surface roughness in the milling process.

2. Experimental procedure

2.1. Characteristics of examined materials

The experimental research was carried out based on two types of materials: microcrystalline CP titanium Grade 2 and high purity nanocrystalline titanium (Table 1).

TABLE. 1

The characterization of examined materials

Material	Short name	Ti content, wt. %
Microcrystalline CP titanium	micro-Ti	~98.9
Nanocrystalline high purity titanium	nano-Ti	99.99

Nanocrystalline titanium (nano-Ti) was produced by hydrostatic extrusion method (HE). HE experiments

* RZESZOW UNIVERSITY OF TECHNOLOGY, DEPARTMENT OF MANUFACURING TECHNIQUE AND AUTOMATION, 12. POWST. WARSZAWY AV., 35-959 RZESZOW, POLAND

** RZESZOW UNIVERSITY OF TECHNOLOGY, DEPARTMENT OF MATERIALS SCIENCE, 12. POWST. WARSZAWY AV., 35-959 RZESZOW, POLAND

*** WARSAW UNIVERSITY OF TECHNOLOGY, FACULTY OF MATERIALS SCIENCE AND ENGINEERING, 141 WOLOSKA STR., 02-507 WARSZAWA

Correspondence author: witekhab@prz.edu.pl.

TABLE. 2

The characteristic of cutting tool

Tool designation	Tool material	Mill diameter	Corner radius	Helix angle	Number of flutes
UGDE0600A5ARA	KC643M	6 mm	0,2 mm	43°	5

were realized at the Institute of High Pressure Physics, Polish Academy of Sciences, within the framework of a project coordinated by the Faculty of Materials Science and Engineering, Warsaw University of Technology.

Initially high purity titanium was in the form of the rod with the diameter of Ø50 mm. This material was subjected to the multi-pass hydrostatic extrusion process. 10 passes of the hydrostatic extrusion process at the room temperature were conducted during which the rod diameter was gradually reduced. The final rod diameter was Ø7 mm.

The material before extrusion was characterized by irregular, fine-crystalline grains. No inclusions were observed <Fig. 1a>. The transmission electron microscopy observations of the Ø7 mm rod have revealed the grain refinement of the initial microstructure <Fig. 1b>. On the transverse section, based on the image analysis methods, the average grain size in the extruded material was found to be about 110 nm.

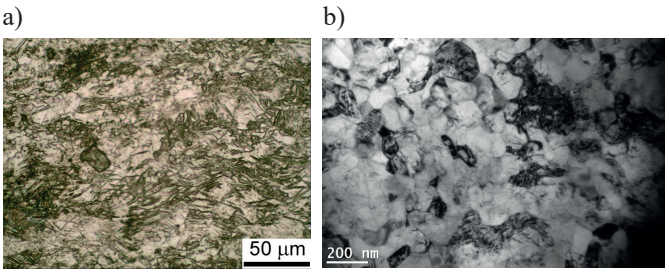

Fig.1. Microstructure of high purity titanium rod: a) before and b) after hydrostatic extrusion

2.2. Test stand and cutting condition

The tests was carried out on test stand prepared with a use of high precision, 5-axis milling machine Ultrasonic 20 Linear <Fig. 2>. This machine tool allows micro machining with high dimensional accuracy. The sample was mounted directly on Kistler 9256C2 dynamometer, which was screwed to the rotary table in the milling machine.

Fig. 2. Sample fixed to dynamometer on the Ultrasonic 20 Linear milling machine

A proper cutting tool material and coating selection also plays an important role in titanium alloys machining [15]. For the process end mill UGDE0600A5ARA made of KC643M carbide was used. Characteristic dimensions of end milling cutter <Fig. 3><Tabl. 2>: D1=6 mm; D=6 mm; Ap1 max=18 mm; L=63 mm; Re=0,2 mm.

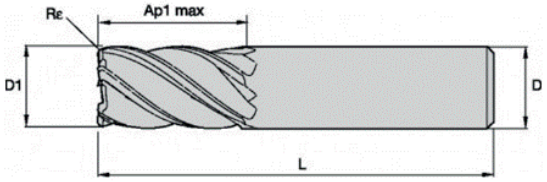

Fig. 3. The geometry of end mills UGDE

The analysis of cutting forces and surface roughness for the shoulder face milling process of pure micro- and nanocrystalline titanium required selection of the specific research area. The range of machining parameters which was applied during the research of cutting force components was determined on the basis of initial investigations and the recommendations of tool manufacturer <Tab. 3>.

TABLE 3

The range of machining parameters

Parameter	Unit	Range
Cutting speed v_c	m/min	40-60
Feed f	mm/tooth	0.009-0.029
Depth of cut a_p	mm	1-2
Width of cut a_e	mm	1.2

Analysis of surface roughness was realized only for feed changes in the adopted range.

2.3. Design of experiment

The response surface methodology (RSM) is a procedure able to determine a relationship between independent input process parameters and output data (process response). The data required to develop the computation were collected by designing the experiments based on Central Composite Design <Tab. 4>. This procedure creates designs with desirable statistical properties. The analysis of results was performed using the Design Expert 8.0.7 software.

3. Results and discussion

In the first step the components of cutting force for specified process conditions were determined. The cutting

TABLE 4

Cutting parameters for Central Composite Design

Levels	-Alpha	Low	Central	High	+Alpha
Coded value	-1.68	-1	0	+1	+1.68
Cutting speed v_c [m/min]	33.18	40	50	60	66.82
Depth of cut a_p [mm]	0.66	1	1.5	2	2.34
Feed rate f [mm/tooth]	0.002	0.009	0.019	0.029	0.036

TABLE 5

The results of cutting force components for the each tests during milling of micro- and nanocrystalline titanium

Std	Factor 1: Cutting speed v_c, m/min	Factor 2: Depth of cut a_p, mm	Factor 3: Feed rate f, mm	Micro-Ti Force F_t, N	Micro-Ti Force F_r, N	Nano-Ti Force F_t, N	Nano-Ti Force Fr, N
1	40	1	0.009	28	22	18	27
2	60	1	0.009	25	24	19	26
3	40	2	0.009	35	41	31	42
4	60	2	0.009	37	48	35	45
5	40	1	0.029	53	36	38	40
6	60	1	0.029	50	36	38	39
7	40	2	0.029	66	81	57	79
8	60	2	0.029	72	77	60	78
9	33.18	1.5	0.019	50	49	44	49
10	66.82	1.5	0.019	47	48	38	48
11	50	0.66	0.019	31	19	29	26
12	50	2.34	0.019	58	73	52	74
13	50	1.5	0.002	18	22	13	23
14	50	1.5	0.036	77	75	61	62
15	50	1.5	0.019	51	51	40	48
16	50	1.5	0.019	47	48	36	48
17	50	1.5	0.019	52	46	37	49
18	50	1.5	0.019	49	52	39	51
19	50	1.5	0.019	41	48	40	54
20	50	1.5	0.019	51	49	39	48

force components measure the resistance of machined material, which has to be overcome during the machining process. In this case, the research aimed at examining to what extent the cutting force components, during machining of microcrystalline and nanocrystalline titanium, differ. The total cutting force F can be decomposed into tangent Ft, radial Fr and axial component Fa. Based on the obtained results, the components Ft and Fr were selected for the comparison. The tangent and axial component of cutting force were calculated on the basis of measurement results obtained from dynamometer (F_X, F_Y, F_Z) and geometric relations presented in Figure 4.

Table 5 shows the values of the cutting force components obtained during the milling of micro- and nanocrystalline titanium.

For adopted modified linear model the analysis of variance ANOVA was performed. The analysis showed that significant effect on the obtained value of the cutting force F_t has feed rate f and depth of cut a_p for both examined materials.

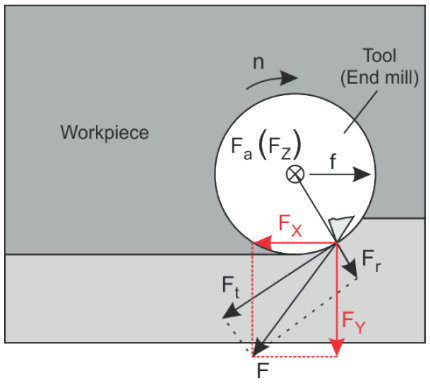

Fig. 4. The relationships between the components of the cutting forces

The result is the mathematical models of tangential component of cutting force Ft for milling process of microcrystalline titanium:

$$F_t = -4{,}675 + 13{,}094 \cdot a_p + 1649{,}177 \cdot f \quad (1)$$

and nanocrystalline:

$$F_t = -9{,}426 + 15{,}916 \cdot a_p + 1250{,}113 \cdot f \quad (2)$$

In Figures 5 and 6 the graphical representation of the above models as a dependence of cutting force Ft on the depth of cut ap and feed rate f consecutively for micro- and nanocrystalline titanium were showed.

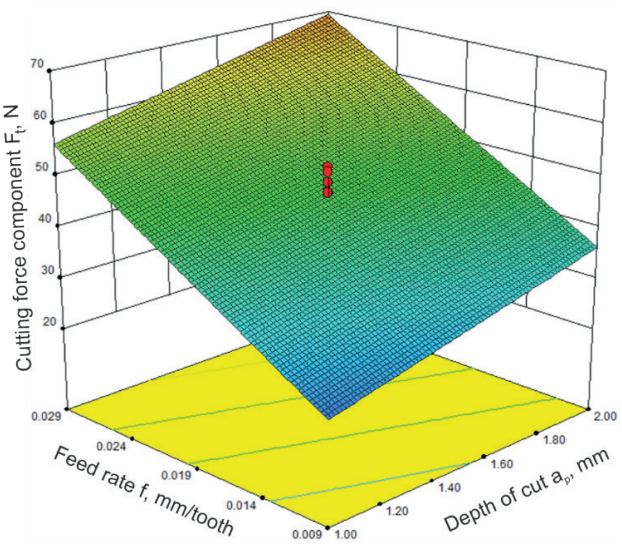

Fig. 5. Effect of feed rate and depth of cut on the tangential force during the milling of microcrystalline titanium (Eq. 1)

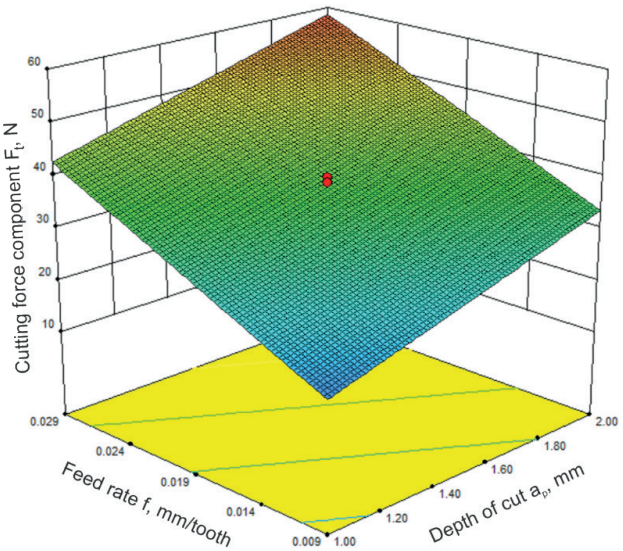

Fig. 6. Effect of feed rate and depth of cut on the tangential force during the milling of nanocrystalline titanium (Eq. 2)

The tangent force was obtained in the range of 18-77 N for microcrystalline titanium and in range of 13-61 for nanocrystalline titanium. The values of tangent component of cutting force Ft during the milling process of nanocrystalline titanium are lower (in the range to 40%) than in the case of its microcrystalline form.

Analysis of the radial component of cutting force was carried out as for tangential force. For adopted modified 2FI model the analysis of variance ANOVA was performed. The analysis showed that significant effect on the obtained value of the radial force F_r has feed rate f, depth of cut ap and interaction between these parameters for both examined materials.

The result is the mathematical models of radial component of cutting force F_r for milling process of microcrystalline titanium:

$$F_r = 3{,}983 + 11{,}766 \cdot a_p - 264{,}203 \cdot f + 1075 \cdot a_p \cdot f \quad (3)$$

and nanocrystalline:

$$F_o = 14{,}333 + 7{,}324 \cdot a_p - 466{,}785 \cdot f_z + 1100 \cdot a_p \cdot f_z \quad (4)$$

In Figures 7 and 8 the graphical representation of the above models as a dependence of cutting force F_r on the depth of cut ap and feed rate f consecutively for micro- and nanocrystalline titanium were showed.

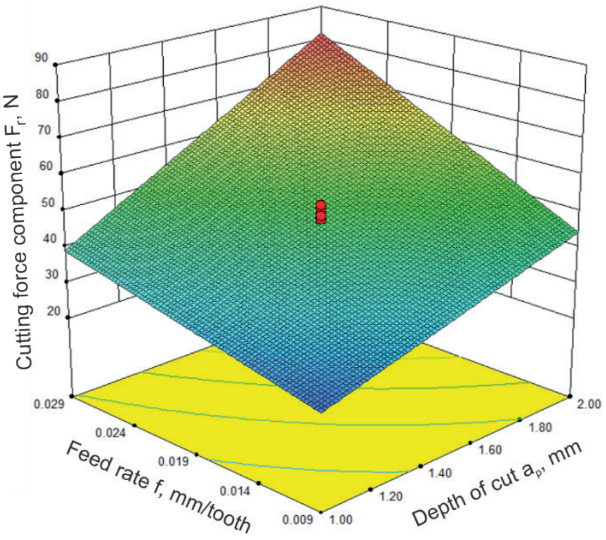

Fig. 7. Effect of feed rate and depth of cut on the radial force during the milling of microcrystalline titanium (Eq. 3)

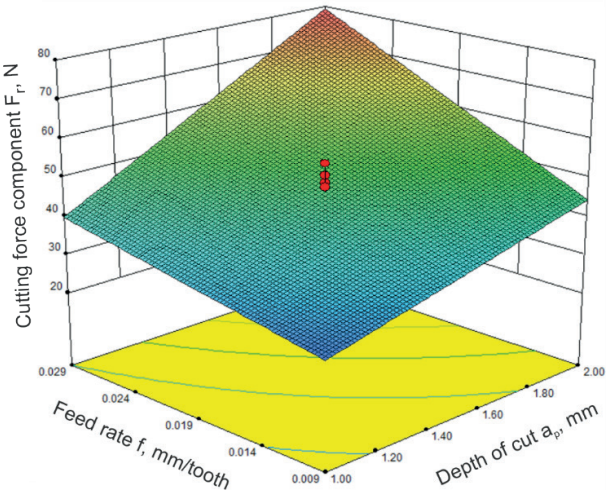

Fig. 8. Effect of feed rate and depth of cut on the radial force during the milling of nanocrystalline titanium (Eq. 4)

The radial force was obtained in the range of 19-81 N for microcrystalline titanium and in range of 23-79 for nanocrystalline titanium. The values of radial component of cutting force showed no significant differences in the adopted range of cutting parameters.

Fig. 9 presents images of the surface topography after face milling. In the case of microcrystalline titanium surface images show a dependence on feed rate. For nanocrystalline titanium the machining traces are more similar.

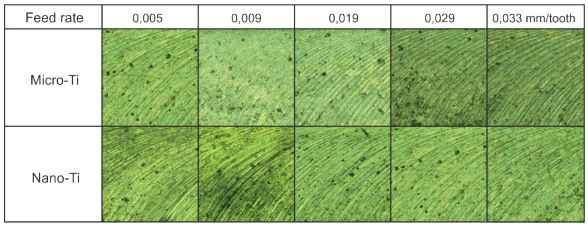

Fig. 9. Surface topography after face milling for different feed rate

For face milling, the results of surface roughness show that parameters Sa and Sz obtained during the milling of nanocrystalline titanium are greater than for microcrystalline titanium surface machined with the same cutting conditions <Fig 10,11>.

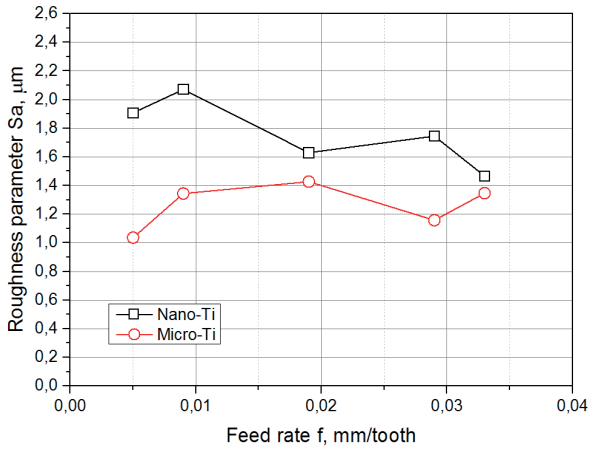

Fig. 10. The impact of feed on the roughness parameter Sa for face milling

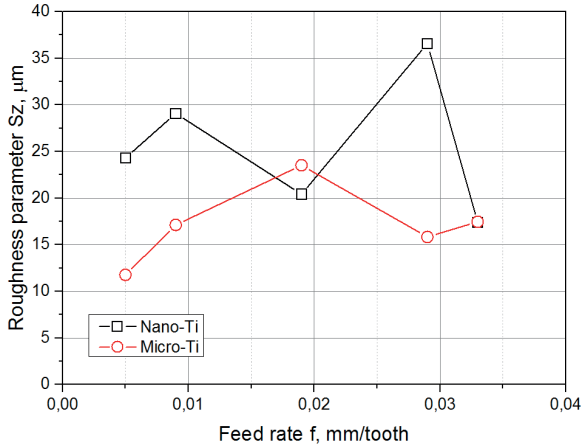

Fig. 11. The impact of feed on the roughness parameter Sz for face milling

The obtained value of surface roughness parameters present a rather complex nature of the forming of surface roughness during the milling of nanocrystalline titanium. The inverted trend of the parameter Sa for face milling of nanocrystalline titanium was observed. With the increase of feed fate the value of Sa parameter was decreased.

The images of surface topography after the side milling are presented on Fig. 12. The machining traces for nanocrystalline titanium depend on feed rate.

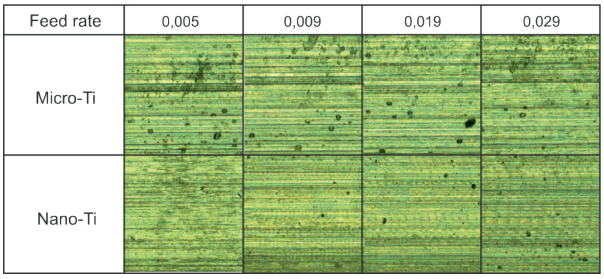

Fig. 12. Surface topography after side milling for different feed rate

As for face milling, the results of surface roughness for side milling presents the same trend. The obtained roughness parameters Sa and Sz during the milling of nanocrystalline titanium are greater than for microcrystalline <Fig. 12, 13>. The significant impact of feed rate on the roughness parameters for side milling was not determined.

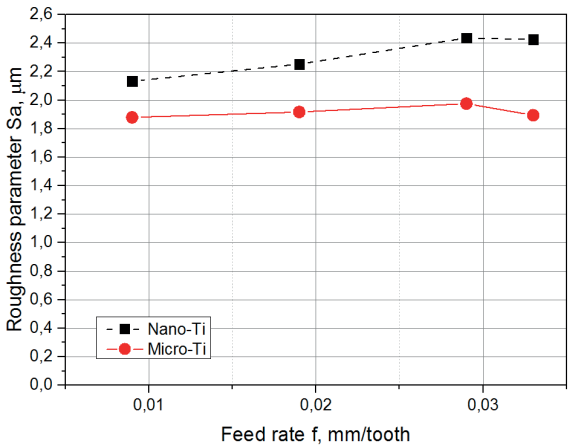

Fig. 13. The impact of feed rate on the roughness parameter Sa for side milling

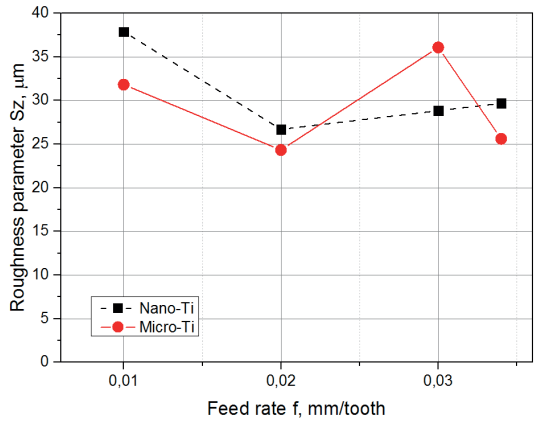

Fig. 14. The impact of feed rate on the roughness parameter Sz for side milling

4. Conclusions

The values of tangential component of cutting force Ft during the milling process of nanocrystalline titanium are lower to 40% than for its microcrystalline form. The comparison of value of radial component Fr does not show significant differences between obtained results.

The research enabled to elaborate models of tangential and radial components of cutting force for milling process of micro- and nanocrystalline titanium. The models of the components of cutting forces show a significant impact of depth of cut and feed rate in the analysed range of cutting parameters.

In the case of machining of nanocrystalline titanium, the determined values of roughness parameter Sa are higher than 15 to 24% than for microcrystalline titanium. The inverted trend of the parameter Sa for face milling of nanocrystalline titanium was observed (in the adopted range of machining parameters). Analysis presents a rather complex nature of the forming of surface roughness during the milling of nanocrystalline titanium.

The subject of further investigations should be determination if the change in forming process of surface topography occurred for lower feed parameters, also a comparison with the results of surface topography measurements obtained by a contact method (only optical method could be used for the geometry of applied sample, which could influence the accuracy of measurement).

Acknowledgement

Financial support of Structural Funds in the Operational Program – Innovative Economy (IE OP) financed by the European Regional Development Fund – Project No POIG.01.03.01-00-015/08 (NANOMET) is gratefully acknowledged.

REFERENCES

[1] K. Topolski, W. Pachla, H. Garbacz, Progress in hydrostatic extrusion of titanium, Journal of Material Science **48**, 4543-4548 (2013).

[2] K. Topolski et al., Mechanical Properties of nanocrystalline titanium fabricated by hydrostatic extrusion, Archives of Metallurgy and Materials **57**, 863-867 (2012).

[3] N. Narutaki, A. Murakoshi, S. Motonishi, H. Takeyama, Study on Machining of Titanium Alloys, CIRP Annals - Manufacturing Technology **32**, 65-69 (1983).

[4] C. Veiga, J.P. Davim, A.J.R. Loureiro, Review on machinability of titanium alloys: the process perspective, Reviews on Advanced Materials Science, **34**, 148-164 (2013).

[5] G. Krolczyk, P. Nieslony, S. Legutko, S. Hloch, I. Samardzic, Investigation of selected surface integrity features of duplex stainless steel (DSS) after turning, Metalurgija **54**, 1, 91-94 (2015).

[6] E.O. Ezugwu, J. Bonney, Y. Yamane, An overview of the machinability of aeroengine alloys, Journal of Materials Processing Technology **134**, 233-253 (2003).

[7] D.I. Lalwani N.K. Mehta, P.K. Jain, Experimental investigations of cutting parameters influence on cutting forces and surface roughness in finish hard turning of MDN250 steel, Journal of Materials Processing Technology **206**, 167-179 (2008).

[8] M.W. Aziziet al., Surface roughness and cutting forces modeling for optimization of machining condition in finish hard turning of AISI 52100 steel, Journal of Mechanical Science and Technology, **26**, 4105-4114 (2012).

[9] G. Bartarya, S.K. Choudhury, Effect of Cutting Parameters on Cutting Force and Surface Roughness During Finish Hard Turning AISI52100 Grade Steel, Procedia CIRP, **1**, 651-656 (2012).

[10] M. Donachie, Titanium: a technical guide (Metals Park, OH: American Society for Metals, 1988).

[11] S. Jaffery and P. Mativenga, Assessment of the machinability of Ti-6Al-4V alloy using the wear map approach, The International Journal of Advanced Manufacturing Technology **40**, 687-696 (2009).

[12] A.R. Zareena, S.C. Veldhuis, Tool wear mechanisms and tool life enhancement in ultra-precision machining of titanium, Journal of Materials Processing Technology **212**, 560-570 (2012).

[13] K.V. Kutniy et al., Obtaining of pure nanostructured titanium for medicine by severe deformation at cryogenic temperatures, Materialwissenschaft Und Werkstofftechnik **42**, 114-117 (2011).

[14] R. Lapovok, A. Molotnikov, Y. Levin, A. Bandaranayake, Y. Estrin., Machining of coarse grained and ultra fine grained titanium, Journal of Materials Science **47**, 4589-4594. (2012).

[15] D. Ulutan, T. Ozel, "Machining induced surface integrity in titanium and nickel alloys: A review, International Journal of Machine Tools and Manufacture **51**, 250-280 (2011).

[16] E.O. Ezugwu, Z.M. Wang, Titanium alloys and their machinability a review, Journal of Material Processing Technology **68**, 262-274 (1997).

[17] K.E. Oczos, Ksztaltowanie ubytkowe tytanu i jego stopów w przemysle lotniczym i technice medycznej, Mechanik **8-9**, 639-656 (2008).

[18] H. Ding, Y.C. Shin, Dislocation density-based grain refinement modeling of orthogonal cutting of commercially pure titanium, Proc. of ASME 2011 Int. Manufacturing Science and Engineering Conference, MSEC 2011-50220, 1-10.

[19] P. Nieslony, G. Wit, P. Laskowski, W. Habrat, FEM-based modelling of the influence of thermophysical properties of work and cutting tool materials on the process performance, Procedia CIRP **12**, 3-8 (2013).

[20] L. Wen-Hsiang, Modeling of cutting forces in end milling operations, Tamkang Journal of Science and Engineering, **3**, 15-22 (2000).

[21] G.M. Krolczyk, P. Nieslony, S. Legutko, Determination of tool life and research wear during duplex stainless steel turning, Archives of Civil and Mechanical Engineering,**15**, 347-354 (2015).